

Model Predictive Control for Renal Anemia Treatment through Physics-informed Neural Network

Zhongyu Zhang* Zukui Li*

* Department of Chemical & Materials Engineering, University of Alberta, Edmonton, T6G 1H9, Canada (e-mail: zhongyu4@ualberta.ca; zukui@ualberta.ca).

Abstract: Patients with chronic kidney disease suffer from renal anemia due to inadequate erythropoietin (EPO) secretion. Determining the optimal EPO dosage and frequency is complex and requires decision-support technologies. Model predictive control (MPC) is an effective decision-making technique that requires a prediction model of the controlled process. In this work, it was discovered that Physics-Informed Neural Networks for Control (PINNC), which integrates physiological model with data-driven methodology, were capable of predicting the patient hemoglobin level with good accuracy and computational efficiency. Based on this prediction model, we developed a zone MPC framework to optimize the dosing strategy. Simulation results show that the proposed control method can serve as an effective tool for determining the optimal EPO dosages for renal anemia patients.

Keywords: Renal anemia; Erythropoietin therapy; Model predictive control; Physics-informed neural networks

1. INTRODUCTION

Patients with chronic kidney disease often experience renal anemia due to inadequate secretion of erythropoietin (EPO) (Babitt and Lin, 2012). The treatment for this condition involves the administration of recombinant human EPO, which is typically prescribed based on hemoglobin (Hgb) levels and previous dosage records. However, determining the optimal EPO frequency and dosage is a complex task that requires extensive clinical experience. This is because while low Hgb levels can lead to anemia, excessive Hgb levels can increase the risk of Hgb fluctuations and even mortality (Bradbury et al., 2009). Thus, it is essential to provide medical staff with decision-support technologies that can assist in determining the optimal EPO dosage and frequency to maintain desired Hgb levels and minimize treatment costs.

Model predictive control (MPC) is used in this work to determine the optimal EPO dosage for anemia treatment. Based on receding-horizon optimization, classical MPC is designed to achieve a set-point target, which is appropriate for systems that need to follow specific trajectories. However, many practical control problems require keeping the desired state within a defined zone, rather than a specific value. This type of target zone is frequently required in biomedical control systems, such as the regulation of blood glucose levels and Hgb levels. In such cases, it is possible to integrate the target zone into MPC by using Zone Model Predictive Control (ZMPC) (Grosman et al., 2010). ZMPC divides the trajectory into two parts: permitted ranges and undesired areas. The objective of ZMPC is to manipulate

the EPO dosages so that the Hgb levels stay within the permitted ranges. The block diagram of the ZMPC system for Hgb control is presented in Figure 1.

Physics model and data-driven model are widely used in predictive control. Physics models are based on fundamental principles and can provide a deep understanding of the underlying mechanisms that govern a system, while data-driven models can capture complex relationships and patterns in data that may not be readily apparent through physical models alone. In the context of regulating human Hgb levels, physiological model may not fully capture the complexities of real patient. On the other hand, relying solely on a data-driven approach may struggle with inaccuracies because of data deficiencies or poor clinical data quality. The convergence of physics-based models and data-driven approaches, however, presents a promising avenue, offering a more potent and adaptable framework for predicting and controlling human hemoglobin levels with improved accuracy and applicability. Introduced by Raissi et al. (2019), physics-informed neural networks (PINN) is a type of machine learning technique that combines the power of neural networks with the physical laws that govern the system. This is achieved by adding penalty terms on physical law (model equation) violations to the loss function for neural network training. This combination can regularize the learning process and improve the performance of neural networks. In control applications, PINN can be used to model and control complex systems that may be difficult to model using traditional physics-based models. Using PINN, we can learn from data and incorporate prior knowledge of the system's physics to make predictions. This allows the PINN to be trained on

* Financial support from Natural Sciences and Engineering Research Council of Canada is gratefully acknowledged.

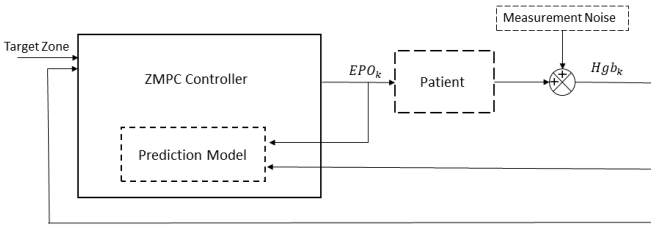


Fig. 1. ZMPC structure

limited data, reducing the need for expensive and time-consuming data collection.

Using PINN in MPC can improve the accuracy and efficiency of the control algorithm, especially in systems with complex or nonlinear dynamics. However, the original PINN does not have interfaces for control input. Besides, the initial states are fixed in one value, which does not meet the requirement for rolling optimization in MPC. Considering these limitations, we apply a modified PINN structure called Physics-Informed Neural Nets for Control (PINNC) (Antonelo et al. (2024), Nicodemus et al. (2022)) in the controller design. The inputs of PINNC consist of time, initial states and control input, making it suitable for MPC implementation. Furthermore, we proposed an approximate exponential function to address impulse inputs and modified PINNC network structure to address time delay in differential equations. To mitigate the challenge of limited training data, we introduced a method for generating augmented training data, aiming to counteract noise in clinical data and enhance the training of neural networks. Additionally, we showcased the remarkable computational efficiency of PINNC within the ZMPC architecture, affirming its capacity for EPO dosage optimization for individualized anemia treatment.

2. PHYSIOLOGICAL MODEL

In this work, we developed the PINN model based on pharmacokinetic and pharmacodynamic model proposed by Chait et al. (2013). The model describes the relationship between Hgb responses and EPO dosages. The model are defined as a pharmacokinetic (PK) model described by Equations 1-4, and a pharmacodynamic (PD) model, described by Equations 5-8

$$\frac{dE(t)}{dt} = -\frac{V \cdot E(t)}{K_m + E(t)} - \alpha \cdot E(t) + dose(t) \quad (1)$$

$$E_p(t) = E(t) + E_{en} \quad (2)$$

$$k_{in}(t) = \frac{S \cdot E_p(t)}{C + E_p(t)} \quad (3)$$

$$E_{en} = \frac{C \cdot H_{en}}{\mu \cdot K_H \cdot S - H_{en}} \quad (4)$$

$$\frac{dR(t)}{dt} = k_{in}(t - D) - \frac{4x_1(t)}{\mu^2} \quad (5)$$

$$\frac{dx_1(t)}{dt} = x_2(t) \quad (6)$$

$$\frac{dx_2(t)}{dt} = k_{in}(t - D) - \frac{4x_1(t)}{\mu^2} - \frac{4x_2(t)}{\mu} \quad (7)$$

$$Hgb(t) = K_H \cdot R(t) \quad (8)$$

In the PK model equations, $E(t)$ denotes the amount of exogenous recombinant human EPO, E_{en} denotes the

endogenous EPO, $E_p(t)$ is the total EPO in plasma, $k_{in}(t)$ is the red blood cells (RBC) production rate, and $dose(t)$ is the EPO dosing in international unit (IU) which is modeled as a train of impulses (Ren et al., 2017). Additionally, the model contains some parameters: H_{en} is the Hgb level due to endogenous EPO, μ represents the mean RBC life span, V is the maximum exogenous EPO clearance rate, K_m stands for the exogenous EPO level that produces half-maximum clearance rate, α is the linear clearance constant, S represents the maximal RBC production rate stimulated by EPO, C is the amount of EPO that produces half-maximum RBC production rate (McAllister et al., 2018).

In the PD model, states $R(t)$ represent the population of red blood cells, states $x_1(t)$ and $x_2(t)$ are internal states that aid in calculating $R(t)$, $Hgb(t)$ is the Hgb level which can be clinically measured, parameters D is the time required for EPO-stimulated RBCs to start forming, K_H is the average amount of Hgb per RBC (mean corpuscular Hgb, or MCH, in a complete blood count) which takes the value of $K_H = 29.5pg/cell$ (McAllister et al., 2018).

In addition to the use in PINN modeling, the above PK/PD model is also used as the basis of the patient simulator in this work. This is achieved through numerically solving the delayed differential equations (DDE).

3. PHYSICS-INFORMED NEURAL NETWORKS FOR CONTROL

PINN model can incorporate the physical model equations in data-driven models to improve interpretability and predictive power of neural networks. Notice that for the conventional PINN, the initial conditions are fixed. If control inputs appears in the model, they are also fixed. As a result, the PINN model can not handle the case with varying initial conditions and control inputs. Hence, it is not qualified for MPC application.

The physics informed neural network for control (PINNC) was proposed by Antonelo et al. (2024). Compared with original PINN, the modified PINNC has two more inputs for control action u and initial conditions. As initial conditions and control actions change with each rolling optimization, the proposed PINNC can generate model predictions based on these inputs. The output of this network is given by Equation 9.

$$\hat{x}(kT + t) = f^{NN}(t, x(kT), u(kT)), t \in [0, T] \quad (9)$$

It's worth noting that in PINNC, we consider multiple equidistant time intervals, each interval is represented by $[kT, (k+1)T]$. Traditional PINN tends to degrade rapidly for long time intervals and can only accept input t in the time duration of the training data (Antonelo et al., 2024). Through the shorter period of T , PINNC solves this degradation problem. Given the initial condition $x(kT)$ and input $u(kT)$, all the states during this time interval can be predicted by trained PINNC. After getting $x((k+1)T)$, we can use the final states as new initial states for next time interval and repeat this process iteratively.

There is a delay in the impact of the EPO input on the Hgb response, necessitating the inclusion of previous EPO dosages in addition to the current dosage for the neural network. In general, for the differential equations with

input delay defined by Equation 10, the neural network structure can be designed as Figure 2.

$$\frac{dx}{dt} = f(t, x(t), u(t), \dots, u(t - \tau T)) \quad (10)$$

For simplicity in expression, consider a scalar state

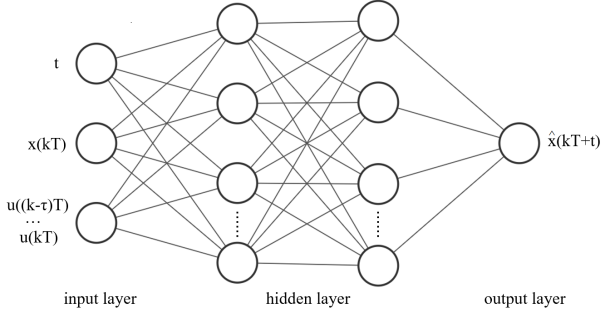


Fig. 2. PINNC architecture to handle delay

variable x and a single ODE equation, the corresponding loss function is a combination of two parts through user-specified weights w^{data} and w^{ode} as follows.

$$Loss(\theta) = w^{data} Loss^{data}(\theta) + w^{ode} Loss^{ode}(\theta) \quad (11)$$

where

$$Loss^{data}(\theta) = \frac{1}{N^{data}} \sum_{n=1}^{N^{data}} (y(t_n) - \hat{x}(t_n, x_n, u_n; \theta))^2 \quad (12)$$

$$Loss^{ode}(\theta) = \frac{1}{N^{ode}} \sum_{n=1}^{N^{ode}} \left(\left. \frac{d\hat{x}}{dt} \right|_{\tau_n} - f(\hat{x}(\tau_n, x_n, u_n; \theta), \tau_n) \right)^2 \quad (13)$$

where (t_n, y_n) , $n = 1, \dots, N^{data}$ are collected data points with y_n being the state measurement value, where τ_n , $n = 1, \dots, N^{ODE}$ are sampled time points for model residual evaluation without corresponding measurement data. Related study has shown that, if the differential equations can represent process system accurately, it is sufficient for training dataset to contain only the initial conditions (Antonelo et al., 2024). But taking full advantage of additional data into loss function can accelerate convergence and improve accuracy of neural network. The automatic differentiation is also employed for calculating the residuals of model equations.

4. HGB PINNC MODELING AND ZMPC

4.1 Modified PK equation for PINNC Modeling

To build a PINNC model based on the PK/PD model Equations 1-8, there is an issue that the impulse input differential Equation 1 cannot be directly used to calculate the residual, and approximating this non-smooth model residual function through neural networks is inefficient. To address this issue, we proposed an approximate analytical approximation solution (Equation 14) for the differential equation 1. This equation describes the decay process of exogenous EPO in the human body, where a_0, a_1, a_2, a_3 are undetermined parameters, t_j and $dose_j$ correspond to the j -th EPO administration time and dosage value,

respectively. $N(t)$ is the total number of dosing times up to time t .

$$E(t) = \sum_{j=1}^{N(t)} dose_j \cdot \exp \left[-\left(a_0 e^{-\frac{dose_j}{a_1}} + a_2 \right) (t - t_j)^{a_3} \right] \quad (14)$$

4.2 Training Data Generation

Our strategy for training the PINNC model involves the generation of augmented training data derived from clinical data, driven by two primary considerations.

Firstly, clinical record data often exhibit measurement noise and disturbances that pose challenges in effectively training the neural network using only clinical Hgb and EPO dosages data. Moreover, exceptional situations such as internal bleeding, blood transfusion, infections, and iron absorption, which are not accounted for in the PK/PD model equations, introduce further complexities into the training process (Chait et al., 2013).

Secondly, clinical data typically lacks information on variables x_1 and x_2 , which could enhance the training of the PINNC model (Wang et al., 2017). To address these issues, we begin by collecting a clinical dataset encompassing EPO dosage values and Hgb records. Subsequently, we employ the inverse PINN method proposed by Zhang and Li (2023) to estimate the unknown parameters of the PK/PD model from the clinical data. Finally, with the estimated PK/PD model parameters, we numerically solve the model equations (Equations 1-8) to obtain simulated data on Hgb, x_1 , and x_2 for use as training datasets.

4.3 Loss function for training

With the collected clinical data for anemia patient and the augmented training data generated using the above procedure, the loss function for PINNC model contains the following terms

$$\begin{aligned} Loss^{data} &= \frac{1}{N^{data}} \sum_{n=1}^{N^{data}} \left\{ (Hgb(t_n) - K_H \cdot \hat{R}(t_n))^2 \right. \\ &\quad \left. + (x_1(t_n) - \hat{x}_1(t_n))^2 + (x_2(t_n) - \hat{x}_2(t_n))^2 \right\} \quad (15) \\ Loss^{ode} &= \frac{1}{N^{ode}} \sum_{n=1}^{N^{ode}} \left\{ \left(\left. \frac{d\hat{x}_1(t)}{dt} \right|_{\tau_n} - \hat{x}_2(\tau_n) \right)^2 \right. \\ &\quad \left. + \left(\left. \frac{d\hat{R}(t)}{dt} \right|_{\tau_n} - \left\{ k_{in}(\tau_n - D) - \frac{4\hat{x}_1(\tau_n)}{\mu^2} \right\} \right)^2 \right. \\ &\quad \left. + \left(\left. \frac{d\hat{x}_2(t)}{dt} \right|_{\tau_n} - \left\{ k_{in}(\tau_n - D) - \frac{4\hat{x}_1(\tau_n)}{\mu^2} - \frac{4\hat{x}_2(\tau_n)}{\mu} \right\} \right)^2 \right\} \quad (16) \end{aligned}$$

4.4 PINNC-based ZMPC for Hgb Control

Like ordinary MPC, zone-MPC uses rolling optimization to calculate optimal manipulated variables and takes the first control input into action based on recurrent states. The significant part of zone-MPC is the cost function. Instead of driving the model output to a specific set point, the cost function of zone-MPC will penalize the prediction

out of defined zone and allow the model output to stay in the permitted range. The zone-MPC is formulated as following

$$\min \sum_{i=1}^N C_{k+i} \|R_{k+i} - R^{ref}\|_Q^2 + \sum_{j=0}^{N-1} \|\Delta EPO_{k+j}\|_R^2 \quad (17)$$

$$\text{s.t. } C_{k+i} = \begin{cases} 0, & \text{if } Hgb^{LB} \leq K_H R_{k+i} \leq Hgb^{UB} \\ 1, & \text{otherwise} \end{cases} \quad (18)$$

$$R^{ref} = \frac{1}{2K_H} (Hgb^{LB} + Hgb^{UB}) \quad (19)$$

$$X_{k+i} = f^{PINNC}(T, X_{k+i-1}, EPO_{k+i-1}, EPO_{k+i-2}) \quad (20)$$

$$\Delta EPO_{k+j} = EPO_{k+j} - EPO_{k-1} \quad (21)$$

$$0 \leq EPO_{k+j} \leq EPO^{max} \quad (22)$$

where the state variable is $X_{k+i} = \{R_{k+i}, x_{1\ k+i}, x_{2\ k+i}\}$, f^{PINNC} is the prediction model using PINNC, C_{k+i} is a penalty coefficient, which penalizes the prediction out of permitted range. The mean value of two bounds is the reference value in Equation 19. It has been proved by Gondhalekar et al. (2013) that zone-MPC has robustness against plant model mismatch as well as against measurement noise. But because there is no penalty to restrain states in the permitted range, the optimal output may be close to the upper bound or lower bound. To solve this problem, usually we can choose a tighter range than actually desired scope.

5. RESULTS

To evaluate the proposed modeling and control strategy, we designed a virtual patient based on the PK/PD model 1-8, with the model parameters reported in Table 1. With

Table 1. Parameters for PK/PD model

α	K_m	V	C	D	H_{en}	μ	S
0.384	129	497	38.0	5.61	6.15	90.4	0.00565

the virtual patient in place, we were able to generate various control input sequences (EPO dose sequences), use them to generate training data and test the prediction performance of the PINNC model as well as the control performance of ZMPC. To simulate the effects of blood transfusion or infection on the patient's Hgb response, we multiply the red blood cell population $R(t)$ by a parameter A_d . Furthermore, to simulate the noise in clinical blood test data, we add a Gaussian noise to the updated RBC population.

In the training process of the PINNC, the proposed approximate model equation 14 is used to replace equation 1. As detailed in Zhang and Li (2023), we simulate the original Equation 14 to get the profile of $E(t)$ under the a given EPO dose sequence. Afterwards, we sample data from the true solution and then use the least squares method to estimate the parameters in the approximate model equation 14. The corresponding parameters a_0, a_1, a_2, a_3 have been estimated as 2.5, 2760, 0.0572 and 1.73, respectively .

To account for time delays in the equations, the EPO input from the previous period is incorporated into the neural network. The architecture depicted in Figure 2 is employed, with τ set to 1. Considering the Hgb treatment

process, we set the sampling period T as 7 days. The neural network consists of 5 hidden layers, each with 128, 256, 512, 256, and 128 neurons. Additionally, N^{data} is set to 945, and N^{ode} is set to 9450. The *Adam* optimizer is utilized with a learning rate of 0.0001. Following 50000 epochs of training, we attain a suitable PINNC model for MPC implementation.

5.1 PINNC model prediction performance

Before implementing PINNC into MPC, we test the model prediction accuracy through self-loop prediction. In this method, we iteratively apply the model to predict the Hgb profile, relying on the initial state and the provided dosing sequence. The self-loop function can be characterized as follows:

$$\hat{x}((k+1)T) = f(T, \hat{x}(kT), u(kT), \dots, u(kT - \tau T)) \quad (23)$$

In addition, we also compare the self-loop PINNC model with the Long Short-Term Memory (LSTM) network which is a pure data-driven recurrent neural network capable of time series analysis and prediction, proposed by Hochreiter and Schmidhuber (1997). The LSTM network comprises three hidden layers with 64, 128, and 64 neurons, respectively. Based on past 8-week Hgb and EPO data, LSTM network predicts the Hgb value of following week. To mitigate overfitting and improve the generalization ability of LSTM, the sample data is divided into a training set (70%) and a validation set (30%).

The neural network's performance is evaluated across multiple test sets. Figures 3-4 and Table 2 illustrate the self-loop predictions of the PINNC and LSTM networks, along with the corresponding root mean square error (RMSE). In test set 1, we reduce the EPO dosages in the training set by half and compare the model's self-loop predictions with the original PK/PD model solution. The results are presented in Figure 3. In test set 2, we generate a set of random EPO dosages based on the mean and standard deviation of the EPO dosage data in the training set. Figure 4 displays the three predicted Hgb trajectories based on this random input sequence.

Table 2. RMSE for self-loop prediction

	LSTM	PINNC
RMSE (Test1)	0.4918	0.2579
RMSE (Test2)	0.6120	0.3435

In general, the PINNC provides a better prediction accuracy compared to the LSTM. Although there is error accumulation, the solution of the optimal control problem within the MPC framework is robust enough to handle this error for larger time horizons. In addition to its accuracy, the PINNC model also demonstrates superior computational efficiency. Table 3 presents a comparison of the time required to calculate Hgb_{k+1} from Hgb_k using both the explicit Euler method from the PK/PD model, the LSTM network, and the proposed PINNC model. The Euler method employs a step size of 0.01s, and both the recursive calculation of the Euler method and the LSTM network are computationally expensive. Additionally, when the PINNC model is integrated into the MPC framework, there is an added acceleration, as the computation of the gradient with respect to control inputs can be performed

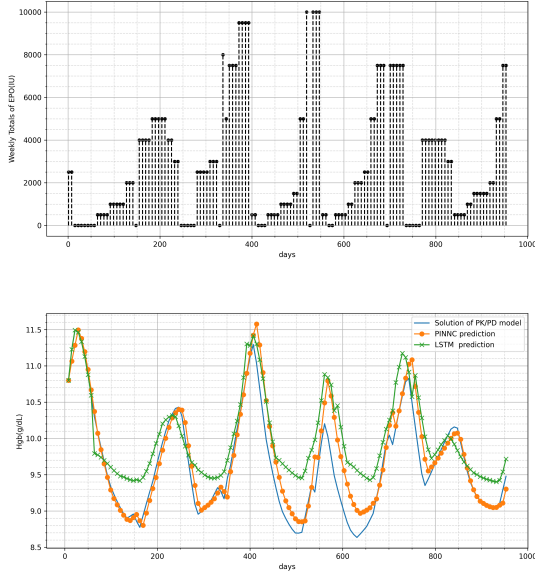


Fig. 3. Test 1: Prediction based on half EPO dosages

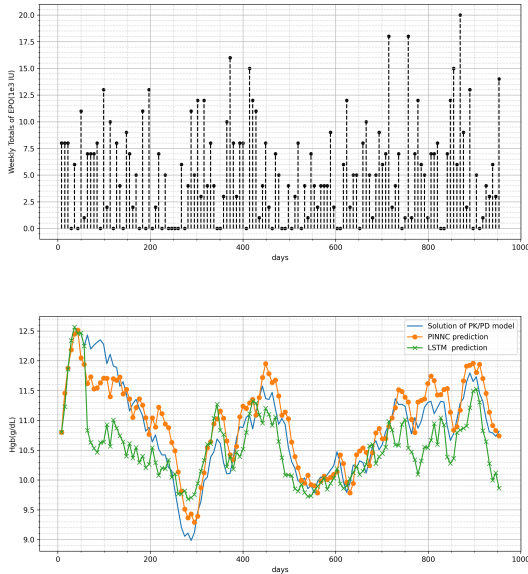


Fig. 4. Test 2: PINNC prediction based on random EPO dosages

Table 3. Execution time for calculating Hgb of next period

	Euler	LSTM	PINNC
Mean execution time (s)	0.0057	0.0179	0.0005

concurrently with the PINNC evaluation, as outlined in Nicodemus et al. (2022).

5.2 Model predictive control results

In clinical treatment, the EPO dosage is within certain ranges. To ensure the safety of the patient, we establish an upper limit on the amount of EPO that can be administered, which is based on the highest recorded EPO

value during the patient’s treatment. This limit is expressed as the inequality constraint 22. For the patient in this experiment, the maximum EPO dosage is 20,000 IU. Considering the healthy range for Hgb (Benz, 2008), we set the target Hgb zone as 13 to 14 grams per deciliter. In addition, we addressed potential complications that may arise during treatment in the previous section, such as internal bleeding and infections. These issues are simulated by multiplying the red blood cell population by a parameter A_d , as described in Equation 24. The parameter A_d assumes a value of 1 in the absence of any abnormal conditions. Nevertheless, at the 175th day, we deliberately assign it a value of 0.8 to emulate the occurrence of internal bleeding, resulting in a abrupt reduction in R_k . In a similar fashion, we modulate A_d to 0.95 between the 525th and 581st days to replicate the presence of a chronic infection. These disturbances increase the realism of the simulation and serve as a test of the model’s robustness.

$$R_{k,new} = A_d R_k \quad (24)$$

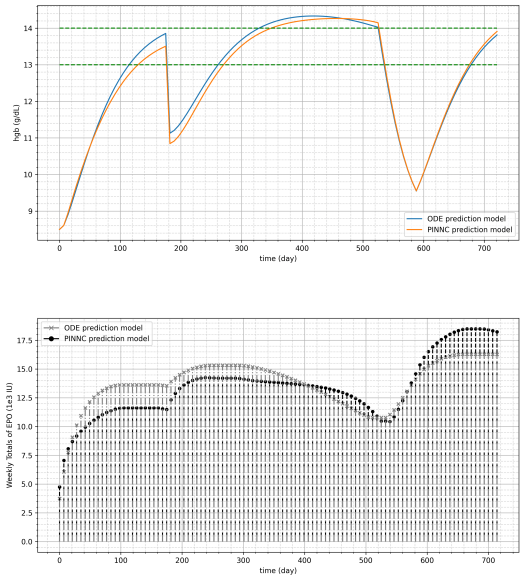


Fig. 5. Solution of ODE-based and PINNC-based zone-MPC with disturbance

The PK/PD Equations 1-8, utilizing the parameters from Table 1, are employed in the virtual patient simulator and solved using the Euler method. The prediction horizon for the system is set at 4 weeks, and the tuning parameters for zone-MPC are configured as $Q = 1000$ and $R = 0.2$. For comparison purposes, we also implement a zone MPC using the same PK/PD model as a prediction model. Its performance is then compared with the PINNC model-based ZMPC. The simulation results spanning a duration of 728 days are presented in Figure 5, indicating that the patient’s Hgb levels, starting at 8.5, stabilize within the healthy range. Despite instances of internal bleeding on the 175th day and an infection between the 525th and 581st day, the controller effectively responds to these disturbances, restoring the Hgb levels to normal.

We also consider the impact of measurement noise in the system. A series of Gaussian noise are added to the Hgb

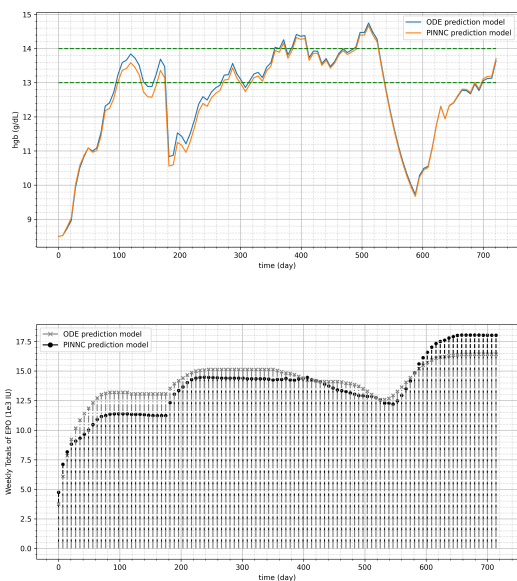


Fig. 6. Solution of ODE-based and PINNC-based zone-MPC with disturbance and noise

measurement from the patient simulator. The mean of the distribution is 0, while the standard deviation is set to 0.3. The combined effect of disturbances and noise is shown in Figure 6. When the Hgb level is within the permissible range, the EPO dosage remains unchanged. However, when the Hgb level approaches the boundary, the controller adjusts the dosage value accordingly. The simulation results demonstrate satisfactory control performance over a two-year period. Furthermore, the simulation results obtained using PINNC closely match the control response based on PK/PD prediction model, confirming that PINNC can serve as a reliable approximation model to replace the physiological model in controller design.

6. CONCLUSION

A key challenge in modeling and controlling the Hgb response is the large variability that exists between individuals. As such, personalized modeling approaches that incorporate patient-specific data and physiological knowledge may be necessary to develop accurate and effective models of the Hgb response. The original PINN can not meet the requirement to update the initial states and control input. Therefore, we propose to use the PINNC as the prediction model. This framework makes PINN suitable for controller design. Meanwhile, this kind of neural network can also use physics information to improve performance. According to the optimized EPO dosage and schedule, patient's Hgb level can be controlled in the target range. The proposed zone-MPC system with PINNC model can serve as a data-driven decision supporting tool for anemia treatment. The proposed modeling approach can be further extended by incorporating patient-specific data, such as the patient's age, gender, and medical history.

REFERENCES

Antonelo, E.A., Camponogara, E., Seman, L.O., Jordanou, J.P., de Souza, E.R., and Hübner, J.F. (2024). Physics-

informed neural nets for control of dynamical systems. *Neurocomputing*, 127419.

Babitt, J.L. and Lin, H.Y. (2012). Mechanisms of anemia in ckd. *Journal of the American Society of Nephrology*, 23(10), 1631–1634.

Benz, E.J. (2008). Disorders of hemoglobin. *Harrison's principles of internal medicine*, 18, 852–61.

Bradbury, B.D., Danese, M.D., Gleeson, M., and Critchlow, C.W. (2009). Effect of epoetin alfa dose changes on hemoglobin and mortality in hemodialysis patients with hemoglobin levels persistently below 11 g/dl. *Clinical Journal of the American Society of Nephrology*, 4(3), 630–637.

Chait, Y., Horowitz, J., Nichols, B., Shrestha, R.P., Hollot, C.V., and Germain, M.J. (2013). Control-relevant erythropoiesis modeling in end-stage renal disease. *IEEE Transactions on Biomedical Engineering*, 61(3), 658–664.

Gondhalekar, R., Dassau, E., Zisser, H.C., and Doyle III, F.J. (2013). Periodic-zone model predictive control for diurnal closed-loop operation of an artificial pancreas. *Journal of diabetes science and technology*, 7(6), 1446–1460.

Grosman, B., Dassau, E., Zisser, H.C., Jovanović, L., and Doyle III, F.J. (2010). Zone model predictive control: a strategy to minimize hyper- and hypoglycemic events. *Journal of diabetes science and technology*, 4(4), 961–975.

Hochreiter, S. and Schmidhuber, J. (1997). Long short-term memory. *Neural computation*, 9(8), 1735–1780.

McAllister, J., Li, Z., Liu, J., and Simonsmeier, U. (2018). Epo dosage optimization for anemia management: Stochastic control under uncertainty using conditional value at risk. *Processes*, 6(5), 60.

Nicodemus, J., Kneifl, J., Fehr, J., and Unger, B. (2022). Physics-informed neural networks-based model predictive control for multi-link manipulators. *IFAC-PapersOnLine*, 55(20), 331–336.

Raissi, M., Perdikaris, P., and Karniadakis, G.E. (2019). Physics-informed neural networks: A deep learning framework for solving forward and inverse problems involving nonlinear partial differential equations. *Journal of Computational physics*, 378, 686–707.

Ren, J., McAllister, J., Li, Z., Liu, J., and Simonsmeier, U. (2017). Modeling of hemoglobin response to erythropoietin therapy through constrained optimization. In *2017 6th International Symposium on Advanced Control of Industrial Processes (AdCONIP)*, 245–250. IEEE.

Wang, J., Perez, L., et al. (2017). The effectiveness of data augmentation in image classification using deep learning. *Convolutional Neural Networks Vis. Recognit*, 11(2017), 1–8.

Zhang, Z. and Li, Z. (2023). Haemoglobin response modelling under erythropoietin treatment: Physiological model-informed machine learning method. *The Canadian Journal of Chemical Engineering*, 101, 4307–4319.